

# Entropy Gradient-based Exploration with Cooperative Robots in 3-D Mapping Missions

Rui Rocha<sup>\*†</sup>, Jorge Dias<sup>\*</sup> and Adriano Carvalho<sup>†</sup>

{*rprocha | jorge*}@*isr.uc.pt*, *asc@fe.up.pt*

<sup>\*</sup>Institute of Systems and Robotics  
Faculty of Sciences and Technology, Univ. of Coimbra  
Pinhal de Marrocos, 3030-290 Coimbra, PORTUGAL

<sup>†</sup>Department of Electrical and Computer Engineering  
Faculty of Engineering, University of Porto  
Rua Dr. Roberto Frias, 4200-465 Porto, PORTUGAL

**Abstract**—Building cooperatively 3-D maps of unknown environments is one of the application fields of multi-robot systems. This article focuses on the exploration problem with multiple robots, starting upon a previously proposed successful distributed architecture. An entropy gradient-based algorithm is used to select exploration viewpoints in the frontier between explored and unexplored regions. The architecture is refined here with a mutual information-based coordination mechanism, whereby each robot selects new exploration viewpoints so that mutual information between robots' individual visible maps is minimized and map's uncertainty is decreased as fast as possible. Results obtained from experiments with real robots equipped with stereo-vision demonstrate how the entropy gradient-based method converges to a map with lower uncertainty.

**Index Terms**—Multi-robot systems, cooperation, 3-D mapping, entropy, exploration, coordination.

## I. INTRODUCTION

Multi-robot systems (MRS) have been widely investigated for the last decade [1]. These systems employ teams of cooperative robots to carry out missions that either cannot be achieved by a single robot, or where a multi-robot solution is more efficient, cost effective, reliable and robust than a single robot. Building a 3-D map of an unknown environment is one of the application fields of MRS.

Robotic mapping addresses the problem of acquiring spatial models of physical environments through mobile robots [2], using range sensors such as cameras or laser range finders. As sensors have always limited range, are subject to occlusions and yield measurements with noise, mobile robots have to navigate through the environment and build the map iteratively. Robots can be used for building fastidious maps of indoor environments [3], but they are particularly useful on mapping missions of hazardous environments for human beings, such as abandoned underground mines [4] or nuclear facilities [5]. Although it is recognized the potential of MRS on such mapping missions, most of the current state-of-the-art is restricted to single robot solutions, with some exceptions [6], [7], [8]. Extensive research has been devoted to SLAM (e.g. [9], [4], [10]), which is not addressed in this article because it is assumed that robots are externally localized.

When a robot or a team of robots explore an unknown environment and build a map, the objective is to acquire as

much new information as possible with every sensing cycle, so that the time needed to completely explore is minimized. Bourgault et al. [11] address the single robot exploration problem as a balance of alternative motion actions from the point of view of information gain (in terms of entropy), localization quality (using SLAM) and navigation cost. Although they include information gain in their strategy, their formulation is computationally heavy and they were only able to use it off-line, for a limited number of proposed destinations. Yamauchi et al. proposed frontier-based exploration [6] whereby robots are driven towards boundaries between open space and unexplored regions. Burgard et al. developed a technique for coordinating a team of robots while they are exploring their environment to build a 2-D occupancy grid [7]. They use the frontier-cell concept [6] and consider a balance between travel cost and utility of unexplored regions, so that robots simultaneously explore different regions. They do not define an architecture for the team and it is not clear how robots should interact and what to communicate to accomplish the proposed coordination. In their seminal work reported in [12], they used entropy minimization to actively localize a robot by minimizing the expected future uncertainty. In [8], robots are arranged in exploration clusters, which group subsets of robots that are able to communicate with each other.

Our approach to multi-robot exploration is closely related to [6] and [7], with three important improvements. Firstly, we use information theory (see section 2) to explicitly represent uncertainty in the grid-based probabilistic model summarized in section 3. Secondly, we use the distributed architecture model proposed in section 4, which restricts the communication among robots to the minimum necessary to share useful sensory data among robots and to coordinate the exploration. Thirdly, we formally define in section 5 the utility of a target viewpoint, whose maximization is accomplished by maximizing the entropy gradient of low coverage, reachable cells (finding frontier-cells [6]), and minimizing mutual information and interference among robots. Section 6 presents experimental results obtained with real robots equipped with stereo-vision and demonstrates how the entropy gradient-based method converges to a map with lower uncertainty. The article ends with conclusions and future work.

## II. ENTROPY AND MUTUAL INFORMATION

Entropy is a general measure for the uncertainty of a belief [13], [14]. Being  $X$  a discrete random variable over a discrete sample space  $\mathcal{S}$ , its entropy  $H(X)$  takes values in the interval  $0 \leq H(X) \leq b$ , where  $b$  is the size of  $\mathcal{S}$ . The quantity  $H(X)$  measures its shortest description (e.g. in bits), being as high as its uncertainty. Hereafter, we use the base 2 for the logarithm and, in this case, entropy is measured in *bits*. Given two discrete random variables  $X$  and  $Y$ , the entropy definition can be extended to compute the joint entropy  $H(X, Y)$  and the conditional entropy  $H(X | Y)$  or  $H(Y | X)$ .

*Mutual information* provides a measure of the reduction of a random variable's uncertainty due to the knowledge of another and it can be defined as

$$I(X; Y) = H(X) - H(X | Y) = H(Y) - H(Y | X) \quad (1)$$

$$= H(X) + H(Y) - H(X, Y). \quad (2)$$

Notice that  $I(X; Y) = I(Y; X)$  and  $I(X; Y) \geq 0$ , where the equality occurs if  $X$  and  $Y$  are statistically independent.

### A. Sets of discrete random variables

The *joint entropy* of a set of discrete random variables  $\mathcal{X} = \{X_1, \dots, X_n\}$  with joint pdf  $p(\mathcal{X}) = p(X_1, \dots, X_n)$  is [14]

$$H(\mathcal{X}) = H(X_1, \dots, X_n) = \sum_{i=1}^n H(X_i | X_1, \dots, X_{i-1}). \quad (3)$$

It can be proved that

$$H(\mathcal{X}) \leq H(X_1) + H(X_2) + \dots + H(X_n) = \sum_{i=1}^n H(X_i), \quad (4)$$

where the equality occurs if all variables in the set  $\mathcal{X}$  are statistically independent. The definition of mutual information given by equation (1) can be generalized to define the *mutual information*  $I(\mathcal{X}^1; \mathcal{X}^2)$  between two sets of random variables  $\mathcal{X}^1 = \{X_1^1, \dots, X_m^1\}$  and  $\mathcal{X}^2 = \{X_1^2, \dots, X_n^2\}$ . It can be proved that

$$\begin{aligned} I(\mathcal{X}^1; \mathcal{X}^2) &= I(X_1^1, \dots, X_m^1; X_1^2, \dots, X_n^2) \\ &= \sum_{i=1}^m \sum_{j=1}^n I(X_i^1; X_j^2 | X_1^1, \dots, X_{i-1}^1, X_1^2, \dots, X_{j-1}^2) \end{aligned} \quad (5)$$

Equation (2) can be generalized to a *relation between joint entropy and mutual information* of two sets of random variables. It can be proved that for any pair of sets of random variables we have

$$I(\mathcal{X}^1; \mathcal{X}^2) = H(\mathcal{X}^1) + H(\mathcal{X}^2) - H(\mathcal{X}^1 \cup \mathcal{X}^2). \quad (6)$$

1) *Sets of independent random variables*: Given equation (4), the joint entropy of the union of sets of independent random variables is

$$H(\mathcal{X}^1 \cup \mathcal{X}^2 \cup \dots \cup \mathcal{X}^n) = \sum_{X_k \in \mathcal{X}^1 \cup \mathcal{X}^2 \cup \dots \cup \mathcal{X}^n} H(X_k), \quad (7)$$

i.e. it is simply the sum of its variables' entropy. Let  $\mathcal{X}$  be a set of statistical independent random variables. Consider two

subsets of *independent random variables*  $\mathcal{X}^1 \subseteq \mathcal{X}$  and  $\mathcal{X}^2 \subseteq \mathcal{X}$ . Using equation (7), equation (6) may be re-written as

$$\begin{aligned} I(\mathcal{X}^1; \mathcal{X}^2) &= H(\mathcal{X}^1) + H(\mathcal{X}^2) - H(\mathcal{X}^1 \cup \mathcal{X}^2) \\ &= \sum_{X_i^1 \in \mathcal{X}^1} H(X_i^1) + \sum_{X_j^2 \in \mathcal{X}^2} H(X_j^2) - \sum_{X_k \in \mathcal{X}^1 \cup \mathcal{X}^2} H(X_k). \end{aligned} \quad (8)$$

All of the terms in the two first sums of equation (8) will be cancelled by the terms in the last sum, except the terms related with variables belonging to both sets. Thus, we have two cases:

$$I(\mathcal{X}^1; \mathcal{X}^2) = \begin{cases} \sum_{X_i \in \mathcal{X}^1 \cap \mathcal{X}^2} H(X_i), & \mathcal{X}^1 \cap \mathcal{X}^2 \neq \emptyset, \\ 0, & \text{otherwise.} \end{cases}, \quad (9)$$

which means that any mutual information between the two sets is due to variables belonging to both sets.

## III. PROBABILISTIC VOLUMETRIC MAP

This section briefly describes the framework proposed in [15], [16]. The 3-D workspace is divided into equal sized voxels with edge  $\epsilon$ ,  $\epsilon \in \mathbb{R}$  and volume  $\epsilon^3$ . The set of all voxels yielded by such division is the 3-D discrete grid  $\mathcal{Y}$ . Given a 3-D point  $\mathbf{x} \in \mathbb{R}^3$ ,  $v(\mathbf{x})$  denotes the voxel  $l \in \mathcal{Y}$  containing the point  $\mathbf{x}$ . Given a voxel  $l \in \mathcal{Y}$ ,  $\mathbf{w}(l) \in \mathbb{R}^3$  denotes the voxel's center coordinates  $[x_l, y_l, z_l]^T$ . The *coverage* of a voxel  $l \in \mathcal{Y}$  is the portion of the the cell which is covered (occupied) by obstacles. It is modeled through the continuous random variable  $C_l$ , taking values  $c_l$  in the interval  $0 \leq c_l \leq 1$ . The tuple  $M_k = (\mathbf{x}_k, \mathcal{V}_k)$  denotes the  $k$ -th batch of measurements, being  $\mathbf{x}_k$  the sensor's position from where measurements are obtained and  $\mathcal{V}_k$  the set of measurements belonging to the batch, provided by the robot's sensor at  $t = t_k$ ,  $t_k \in \mathbb{R}$ ,  $k \in \mathbb{N}$ . The set  $\mathcal{M}_k = \{M_i : i \in \mathbb{N}, i \leq k\}$  is a sequence of  $k$  batches of measurements, corresponding to the period of time  $t_0 \leq t \leq t_k$ , being  $t_0$  the initial time before any batch of measurements. The knowledge about the voxel's coverage  $C_l$ , after  $k$  batches of measurements, is modeled through the pdf  $p(c_l | \mathcal{M}_k)$ ,  $0 \leq c_l \leq 1$ . The *3-D probabilistic map*, after  $k$  batches of measurements, is the set of random variables  $\mathcal{C} = \{C_l : l \in \mathcal{Y}\}$ , described statistically through the set of coverage probability density functions  $\mathcal{P}(\mathcal{C} | \mathcal{M}_k) = \{p(c_l | \mathcal{M}_k) : l \in \mathcal{Y}\}$ . The coverage of each individual voxel is assumed to be independent from the other voxels' coverage and thus  $\mathcal{C}$  is a set of independent random variables.

### A. Voxel's entropy and map's Entropy

A quantized version of the voxel's coverage pdf is used to compute the voxel's discrete entropy<sup>1</sup>. Each coverage continuous random variable  $C_l$ ,  $l \in \mathcal{Y}$  is sampled through a discrete random variable  $C_l^A$  having  $b$  possible outcomes

<sup>1</sup>Although the voxel's coverage is a continuous random variable, we prefer to discretise it and use discrete entropy, because it is always positive.



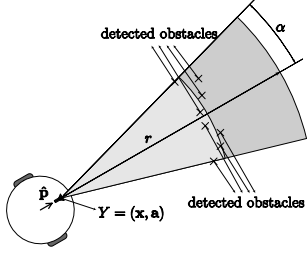


Fig. 2. Robot's visibility represented in 2-D: it is the light-grey shaded region computed upon the maximum range distance  $r$  and the maximum angle  $\alpha$  with the heading  $\hat{\mathbf{p}}$ . Both parameters  $r$  and  $\alpha$  change dynamically with the surrounding environment and, thus, the robot's visibility is smaller than the potential sensor's range (dark-grey shaded region).

the continuous set of points:

$$\mathbf{V}(\mathbf{x}, \mathbf{a}, r, \alpha) = \{\mathbf{y} \in \mathbb{R}^3 : \|\mathbf{y} - \mathbf{x}\| \leq r, \\ 0 \leq \arccos\left(\frac{(\mathbf{y} - \mathbf{x}) \cdot \hat{\mathbf{p}}}{\|\mathbf{y} - \mathbf{x}\|}\right) \leq \alpha\}, \quad (12)$$

with

$$\hat{\mathbf{p}} = [\cos \theta, \cos \phi, \sin \theta, \cos \phi, -\sin \phi]^T. \quad (13)$$

As Fig. 2 shows, the robot's visibility is obviously limited by the sensor's intrinsic nature and its limitations, but it is also limited by the environment surrounding the robot. Whether the robot is currently exploring a wide open area or a narrower space, the robot's visibility is also dynamically conditioned by the presence of obstacles in front of the sensor, which hide the space behind them and reduce the sensor's intrinsic range. In order to dynamically adapt the robot's visibility, we use the latest sensor data to estimate  $r$  and  $\alpha$ . Given the latest batch of  $m_k$  measurements  $M_k = (\mathbf{x}, \mathcal{V}_k)$ , the robot's visibility parameters are estimated as:

$$(\hat{r}, \hat{\alpha}) = \left( \frac{1}{m_k} \sum_{i=1}^{m_k} \|\vec{\mathbf{v}}_{k,i}\|, \max_i \left[ \arccos\left(\frac{\vec{\mathbf{v}}_{k,i} \cdot \hat{\mathbf{p}}}{\|\vec{\mathbf{v}}_{k,i}\|}\right) \right] \right). \quad (14)$$

### B. Visible maps and mutual information

Consider the fleet  $\mathcal{F} = \{1, \dots, n\}$  of  $n$  robots performing a 3-D mapping mission and one of the robots in the team  $i \in \mathcal{F}$ . Its visibility  $\mathbf{V}_i = \mathbf{V}(\mathbf{x}_i, \mathbf{a}_i, r_i, \alpha_i) \subset \mathbb{R}^3$  represents a sub region of the environment that robot  $i$  is able to sense and, thus, measurements gathered from its current pose  $Y_i = (\mathbf{x}_i, \mathbf{a}_i)$  will only influence its knowledge about that sub region. That sub region refers to the subset of voxels

$$\mathcal{Z}^i = \{l \in \mathcal{Y} : \mathbf{w}(l) \in \mathbf{V}(\mathbf{x}_i, \mathbf{a}_i, r_i, \alpha_i)\} \subset \mathcal{Y}. \quad (15)$$

We denote as the *robot's visible map* the subset of coverage random variables

$$\mathcal{C}^i = \{C_l, l \in \mathcal{Z}^i\} \subset \mathcal{C}, \quad (16)$$

which models the robot's knowledge about the visible sub region defined by the voxels  $l \in \mathcal{Z}^i$ . Restricting the sum in

(11) to the set of voxels  $\mathcal{Z}^i$ , the joint entropy of the robot's visible map is

$$H(\mathcal{C}^i) = \sum_{l \in \mathcal{Z}^i} H(C_l) < H(\mathcal{C}), \quad (17)$$

where the inequality means that the robot's visible map covers less uncertainty than the global map's uncertainty.

The other robots in the fleet  $\mathcal{F} \setminus i$  cover the set of voxels

$$\mathcal{W}^i = \bigcup_{j \in \mathcal{F} \setminus i} \mathcal{Z}^j \subseteq \mathcal{Y} \quad (18)$$

and have a joint visible map  $\mathcal{T}^i$  with joint entropy

$$H(\mathcal{T}^i) = \sum_{l \in \mathcal{W}^i} H(C_l) \leq H(\mathcal{C}). \quad (19)$$

The fleet covers the set of voxels  $\mathcal{W} = \mathcal{Z}^i \cup \mathcal{W}^i$  and has a joint visible map  $\mathcal{T} = \mathcal{C}^i \cup \mathcal{T}^i$ . Using equation (6), the *joint entropy of the team's visible map* is given by

$$H(\mathcal{T}) = H(\mathcal{C}^i) + H(\mathcal{T}^i) - I(\mathcal{C}^i; \mathcal{T}^i), \quad (20)$$

which measures the uncertainty being covered by the team. Since both sets of coverage random variables  $\mathcal{C}^i$  and  $\mathcal{T}^i$  are subsets of  $\mathcal{Y}$ , which is a set of independent random variables, the mutual information  $I(\mathcal{C}^i; \mathcal{T}^i)$  between the robot's visible map and the joint visible map of the other robots is given by equation (9): it is null if the robot's visible map does not overlap with the other robots' visible maps; otherwise, it is the sum of the entropy of the voxels belonging to the overlapping.

### C. Multi-robot exploration strategy

In an exploration mission, the objective is to acquire as much new information about the environment as possible with every sensing cycle. Intuitively, this is equivalent to select new regions to explore so that the robot's sensor covers as much uncertainty as possible. That's why the method proposed in [15], [16] aims at maximizing the visible map joint entropy  $H(\mathcal{C}^i)$  of each single robot  $i \in \mathcal{F}$ . However, with multiple robots, the goal of each a robot  $i \in \mathcal{F}$  is to contribute to the maximization of the map's uncertainty  $H(\mathcal{T})$  covered by the team. As equation (20) shows, this is a twofold goal: to maximize the joint entropy of its own visible map  $H(\mathcal{C}^i)$ , likewise in the single robot case; *and* to avoid the overlapping with the other robots' visible maps so that the mutual information  $I(\mathcal{C}^i; \mathcal{T}^i)$  is minimized (see Fig. 3).

Considering a given robot  $i \in \mathcal{F}$ , our exploration method selects the best voxel from a subset of  $\mathcal{Y}$  in its neighborhood, by computing entropy gradient, visible map's mutual information, reachability and occlusions due to other robots. We assume that, whenever a robot  $j \in \mathcal{F}$  selects a new pose  $Y_j^s = (\mathbf{x}_j^s, \mathbf{a}_j^s)$ , all the other robots in the team  $\mathcal{F} \setminus j$  are informed through direct communication about its new selected pose and its current range parameters  $r_j$  and  $\alpha_j$ , i.e. they receive the tuple  $(Y_j^s, r_j, \alpha_j)$ . This minimal communication enables each robot  $i \in \mathcal{F}$  to compute the mutual information  $I(\mathcal{C}^i; \mathcal{T}^i)$  between its visible map  $\mathcal{C}^i$  and the joint visible map of the rest of the team  $\mathcal{F} \setminus i$ .

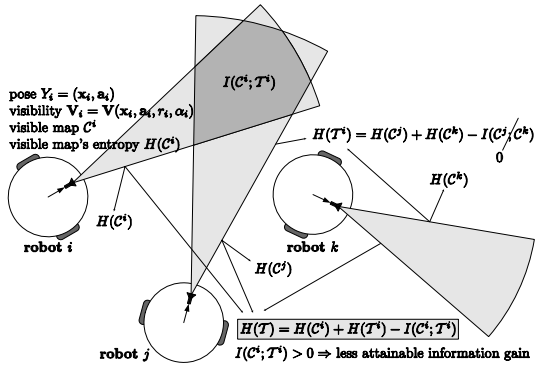


Fig. 3. Example showing visible maps with 3 robots  $i, j$  and  $k$ . The mutual information  $I(\mathcal{C}^i; \mathcal{T}^i) > 0$  decreases the team's visible map joint entropy, i.e. the team covers a smaller part of the map's uncertainty  $H(\mathcal{C})$ .

1) *Subset of voxels in the robot's neighborhood:* As we are mainly interested on ground mobile robots, whose sensor's motion is instantaneously restricted to a plane  $\Gamma$  parallel to the robot's motion plane (e.g. the floor plane), voxels near to plane  $\Gamma$  are preferable to be explored. Consider the current robot's pose<sup>3</sup>  $Y = (\mathbf{x}, \mathbf{a})$ , being  $\mathbf{x}$  its current position and  $\mathbf{a} = \{\theta, \phi, \psi\}$  its orientation. Given a robot's coordinates frame  $\{R\}$ , equal to the global (absolute) coordinates frame  $\{W\}$  after translation and rotation, the robot's sensor motion plane  $\Gamma$  is defined by two orthogonal axes: a longitudinal axis  $\hat{\mathbf{p}}' = [1, 0, 0]^T$ , which is the unitary vector along  $xx$  axis, and a transverse axis  $\hat{\mathbf{q}}' = [0, 1, 0]^T$ , which is the unitary vector along  $yy$  axis; for an UAV,  $\hat{\mathbf{p}}$  would be the axis between tail and head, and  $\hat{\mathbf{q}}$  would be the axis connecting the wings. It can be shown that robot's axes can be expressed in a robot's coordinates frame  $\{R^r\}$ , equal to  $\{W\}$  after translation but without rotation, where  $\hat{\mathbf{p}}$  is given by equation (13) and

$$\hat{\mathbf{q}} = \begin{bmatrix} \cos \theta \cdot \sin \phi \cdot \sin \psi - \sin \theta \cdot \cos \psi \\ \sin \theta \cdot \sin \phi \cdot \sin \psi + \cos \theta \cdot \cos \psi \\ \cos \phi \cdot \sin \psi \end{bmatrix}, \quad (21)$$

Any vector  $\vec{\mathbf{u}}$  can be projected on the robot's sensor motion plane  $\Gamma$  as

$$\text{proj}_{\Gamma} \vec{\mathbf{u}} = (\vec{\mathbf{u}} \cdot \hat{\mathbf{p}})\hat{\mathbf{p}} + (\vec{\mathbf{u}} \cdot \hat{\mathbf{q}})\hat{\mathbf{q}}. \quad (22)$$

Let denote the applied vector connecting the robot's position  $\mathbf{x} \in \mathbb{R}^3$  to the center of voxel  $l$  as

$$\vec{\mathbf{u}}(\mathbf{x}, l) = \mathbf{w}(l) - \mathbf{x}. \quad (23)$$

The new robot's selected position is selected as the center of a voxel from the set of voxels

$$\mathcal{N}_{\Gamma}(\mathbf{x}, r) = \{l \in \mathcal{Y}, \|\vec{\mathbf{u}}(\mathbf{x}, l)\| \leq r, l = v(\text{proj}_{\Gamma} \mathbf{w}(l))\}, \quad (24)$$

in the neighborhood defined by current robot's position  $\mathbf{x}$  and range  $r$ .

<sup>3</sup>Hereafter, the expression *robot's pose* shall be interpreted as the more accurate expression *robot's sensor pose*.

2) *Entropy gradient:* The 3-D grid  $\mathcal{Y}$  discretises the 3-D workspace  $\mathbb{R}^3$  at discrete points  $\mathbf{w}(l)$ ,  $l \in \mathcal{Y}$ , equally spaced by  $\epsilon$  (the voxel's edge). The 3-D map enables us to associate with each of these points an entropy  $H(l) = H(\mathcal{C}_l)$  given by equation (10), therefore we might say that a continuous entropy field  $H : \mathbb{R}^3 \rightarrow \mathbb{R}$  is sampled along the voxels' centers belonging to the grid  $\mathcal{Y}$ . Our volumetric model assumes that each edge of any voxel  $l \in \mathcal{Y}$  is aligned with one of the axes ( $xx$ ,  $yy$  or  $zz$ ) of the global coordinates frame  $\{W\}$ . Let  $l_{\ominus}$  denote the contiguous voxel to  $l$  in the negative direction of axis  $\Theta$ . A reasonable (first order) approximation to the *voxel's entropy gradient* at the center of a voxel  $l$  is

$$\vec{\nabla} H(l) \approx \frac{1}{\epsilon} [H(l) - H(l_{x-}), H(l) - H(l_{y-}), H(l) - H(l_{z-})]^T. \quad (25)$$

The projection of the voxel's entropy gradient on the robot's sensor motion plane  $\Gamma$  is

$$\vec{\nabla} H_{\Gamma}(l) = \text{proj}_{\Gamma} \vec{\nabla} H(l), \quad (26)$$

with magnitude  $\|\vec{\nabla} H_{\Gamma}(l)\|$ . Given that the maximum value of discrete entropy is the number of histogram bins  $b$  in equation (10), and given the gradient approximation yielded by equation (25), the gradient magnitude can be normalized to the interval  $[0, 1]$  as

$$\|\vec{\nabla} H_{\Gamma}(l)\|_N = \frac{\epsilon}{\sqrt{2} \log_2 b} \|\vec{\nabla} H_{\Gamma}(l)\|. \quad (27)$$

If the center of a voxel  $l \in \mathcal{N}_{\Gamma}(\mathbf{x}, r)$  is selected to be the next robot's selected position  $\mathbf{x}^s$ , our method claims that the robot should select the gaze direction  $\mathbf{a}(l)$  defined by the unitary vector

$$\hat{\mathbf{p}}(l) = \frac{\vec{\nabla} H_{\Gamma}(l)}{\|\vec{\nabla} H_{\Gamma}(l)\|}, \quad \vec{\nabla} H_{\Gamma}(l) \neq \vec{0}. \quad (28)$$

3) *Visible map's mutual information:* Before a robot  $i \in \mathcal{F}$  selects its new pose, it can compute the other robots' visibility through equation (12), because, as it was already mentioned, the robot knows  $(Y_j^s, r_j, \alpha_j)$ ,  $\forall j \in \mathcal{F} \setminus i$ . Then, using equations (18) and (19), that robot can compute, respectively, the set  $\mathcal{W}^i$  of visible voxels by the other robots, their joint visible map  $\mathcal{T}^i$  and the joint entropy  $H(\mathcal{T}^i)$ .

Now consider any voxel  $l \in \mathcal{N}_{\Gamma}(\mathbf{x}, r)$  whose center  $\mathbf{w}(l)$  is a candidate point to the robot's next selected position  $\mathbf{x}^s$ , being the new sensor's gaze  $\mathbf{a}(l)$  determined through equation (28). Hereafter, this robot's pose is denoted as  $Y^l = (\mathbf{w}(l), \mathbf{a}(l))$ . The current range parameters  $r$  and  $\alpha$  of the robot's sensor define a visibility region  $\mathbf{V}(\mathbf{w}(l), \mathbf{a}(l), r, \alpha)$ , computed through equation (12). Using equations (15), (16) and (17), the robot computes the visible voxels  $\mathcal{Z}^i(Y^l)$ , the visible map  $\mathcal{C}^i(Y^l)$  and the visible map's joint entropy  $H(\mathcal{C}^i(Y^l))$ , when its pose is  $Y^l$ . Then the mutual information  $I(\mathcal{C}^i(Y^l); \mathcal{T}^i)$  between the visible map from that voxel and the other robots' joint visible map can be computed through equation (9), being equal to the

joint entropy of the intersection voxels  $\mathcal{Z}^i(Y^l) \cap \mathcal{W}^i$ . The non-redundancy coefficient for a candidate voxel is the function  $\lambda : \mathcal{Y} \rightarrow ]0, 1]$ , defined as

$$\lambda(l) = \exp \left[ -\frac{1}{\xi} I(C^i(Y^l); \mathcal{T}^i) \right], \quad (29)$$

where  $\xi$  is a scale factor.

4) *Reachability*: Assuming by simplicity that the robot's path between two consecutive exploration viewpoints is a straight line, the reachability of a given voxel is a function of how much covered are the voxels traversed by the robot when moving its sensor from current pose  $Y = (\mathbf{x}, \mathbf{a})$  to pose  $Y^l$ . These voxels may be either occupied by obstacles in the environment or other robots. Being  $\mathcal{O}(Y, Y^l)$  the traversed voxels by the robot and  $\mathcal{O}^{\mathcal{F} \setminus i}$  the voxels occupied by the rest of the team  $\mathcal{F} \setminus i$ , the *reachability* of a voxel  $l \in \mathcal{N}_\Gamma(\mathbf{x}, r)$  is

$$\rho(\mathbf{x}, l) = \begin{cases} \min_{m \in \mathcal{O}(Y, Y^l)} [1 - E(C_m)], & \mathcal{O}(Y, Y^l) \cap \mathcal{O}^{\mathcal{F} \setminus i} = \emptyset \\ 0, & \text{otherwise} \end{cases}. \quad (30)$$

taking values between 0 (invalid path) and 1 (path completely clear of obstacles).

5) *Occlusions due to other robots*: The presence of other robots within the robot's visibility region yields undesirable occlusions and interference. Using equation (15), the robot computes the visible voxels  $\mathcal{Z}^i(Y^l)$  when its sensor's pose is  $Y^l$ . Let denote as  $\vec{\mathbf{u}}(Y_1, Y_2)$  the vector connecting the center of mass of a robot whose sensor's pose is  $Y_1$  to the center of mass of another robot whose sensor's pose is  $Y_2$ . The non-interference coefficient is the function  $\eta : \mathcal{Y} \rightarrow [0, 1]$ , which we define as

$$\eta(l) = \min_{j \in \mathcal{F}} \begin{cases} \frac{\|\vec{\mathbf{p}}(l) \times \vec{\mathbf{u}}(Y^l, Y_j^s)\|}{r}, & j \neq i \wedge \mathcal{Z}^i(Y^l) \cap \mathcal{O}^j(Y_j^s) \neq \emptyset \\ 1, & \text{otherwise,} \end{cases} \quad (31)$$

where  $\mathcal{O}^j(Y_j^s)$  denotes the set of voxels occupied by robot  $j$ , located in its current selected pose  $Y_j^s$ .

6) *Cost factor*: If we want to reduce the traveled distance during exploration, it is also important to consider the cost associated with each candidate voxel  $l \in \mathcal{N}_\Gamma(\mathbf{x}, r)$ , which is the distance  $\|\vec{\mathbf{u}}(\mathbf{x}, l)\|$  between current robot's position  $\mathbf{x}$  and the center of the candidate voxel  $l$ . We define the cost factor as the function  $\vartheta : \mathbb{R}^3 \times \mathcal{Y} \rightarrow [0, 1]$ , whose expression is

$$\vartheta(\mathbf{x}, l) = \frac{\|\vec{\mathbf{u}}(\mathbf{x}, l)\|}{r}. \quad (32)$$

7) *Determination of the robot's next viewpoint*: Accordingly with our exploration strategy, given the set of voxels  $\mathcal{N}_\Gamma(\mathbf{x}, r)$  in the robot's neighborhood, the robot is directed to the voxel

$$l^s = \operatorname{argmax}_{l \in \mathcal{N}_\Gamma(\mathbf{x}, r)} \left( \left\| \vec{\nabla} H_\Gamma(l) \right\|_{\mathbf{N}} \cdot \lambda(l) \cdot \rho(\mathbf{x}, l) \cdot \eta(l) - \kappa \cdot \vartheta(\mathbf{x}, l) \right). \quad (33)$$

with a gaze on arrival defined by the unitary vector  $\hat{\mathbf{p}}(l^s)$ , computed through equation (28). In the argument of equation (33), the left term measures utility and the right term measures cost, being  $\kappa$  a cost sensitivity coefficient.

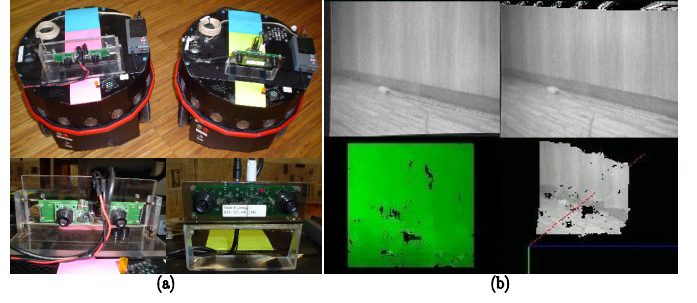


Fig. 4. Robots used in the experiments: (a) Scout mobile robots from Nomadic Technologies (top), equipped with stereo-vision sensors (bottom) and wireless communication; (b) example of a stereo image pair (top) and its respective disparity map (bottom-left) and depth map (bottom-right).

## VI. EXPERIMENTS WITH REAL ROBOTS

The 3-D mapping framework presented in previous sections has been used for carrying out experiments with two real mobile robots in our lab. The mobile robots (see Fig. 4-a) are Scout robots from Nomadic Technologies, having differential kinematics, odometry sensing and sonars. We mounted on the top of both robots a stereo-vision sensor and a modem radio providing wireless TCP/IP communication. Each stereo-vision sensor (see bottom of Fig. 4-a) is a small, compact, low-cost analog stereo rig from Videre Design, with resolution 160x120 pixels. For computing range data from stereo images, we use the Small-Vision System (SVS) v2.3c, a stereo engine from SRI International, which implements an area correlation algorithm for computing range from stereo images, and supports camera calibration, 3-D reconstruction and effective filtering. See Fig. 4-b for an example of a depth map yielded by the SVS engine. Each robot has a ring of 16 Polaroid 6500 sonar ranging modules, which were used for avoiding obstacles when moving the platform, and for preventing the robot to acquire stereo image pairs below a given distance threshold to obstacles.

Fig. 5 depicts a diagram of the software that was built to implement the distributed architecture model of Fig. 1, which is easily scalable to a team having an arbitrary number of robots. There is a host PC for supervision, wherein the user can control the mission execution (e.g. start, pause, restore, stop, etc.) and get access to robots' data (e.g. robots' individual maps, log data, etc.). The host PC is also responsible for providing global localization to the team of robots, through a color segmentation algorithm that detects colored markers on the top of the robots' platforms (see Fig. 4-a).

### A. Results

Fig. 6 shows results obtained within an experiment with the two Scout robots. The mission was to build a 3-D map of a volume in our lab with approximate dimensions  $4.1m \times 4.4m \times 0.7m$ . This volume of approximately  $12.6m^3$  was limited by the floor and existing walls. As the robots' motion was restricted to the floor plane, the upper limit of  $0.7m$  was imposed by the robots' stereo-vision sensors, which had a

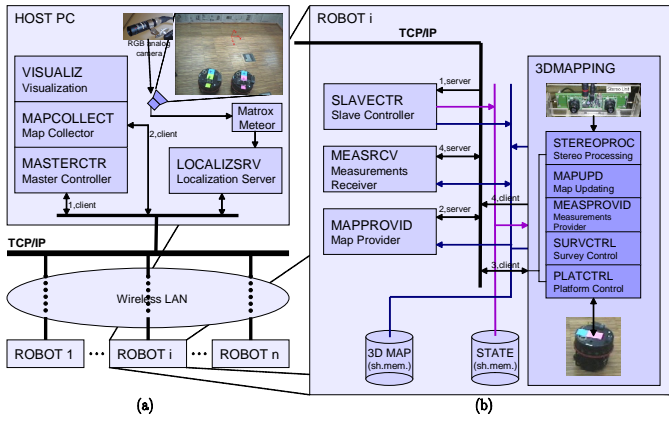


Fig. 5. Diagram of the implemented software in real robots: (a) interaction between the team of robots and a host PC used for supervising 3-D mapping missions and localizing the robots through a global camera; (b) software modules for 3-D mapping, running locally on each robot.

vergence of approximately 12 degrees towards the floor. The entropy of the initial map was  $H(C | \mathcal{M}_0) = 129360$  bits.

The five rows of Fig. 6 represent the map's status of a robot along the mission, at five different instant times  $t_k$  with decreasing values of the map's entropy  $H(C | \mathcal{M}_k)$ . In each row, it is represented in the left column the current 3-D map relative to the world reference frame  $\{W\}$  (red referential), in the middle column the current robot's sensor pose and its next exploration viewpoint, and in the right column a graph of the entropy gradient magnitude  $\|\vec{\nabla} H_{\Gamma}(l)\|_N$  as a function of the  $xy$  coordinates of the voxels' center, for voxels  $l$  that belongs to the robot's sensor motion plane  $\Gamma$ , i.e. voxels that obey the condition  $l \in \mathcal{Y} \wedge l = v(\text{proj } \mathbf{w}(l))$ . The middle column also shows a blue polyline drawn in the floor plane, whose vertexes indicate the sequence of the robot's positions since the beginning of the mission. Comparing the left and right columns, we observe that voxels located at frontiers between explored and unexplored regions have higher values of entropy gradient. Due to equation (33), we can see in the middle and right columns that the robot usually chooses a voxel in its neighborhood with maximum entropy gradient, which yields a robot's visible region with high uncertainty (entropy) and thus high expected information gain. As we can observe in the left column, the entropy gradient-based method converges to a map with lower uncertainty as time  $t_k$  increases.

In the experiment of figure 6, the robots used the coordinated exploration method presented in this article. The experiment was repeated with the uncoordinated version reported in [15], [16]. Comparing both methods, we concluded that the coordinated exploration method: (1) yielded a reduction of 13.4% in the time required by the team to perform the mission; (2) and reduced that time from 72.1% [15], [16] to only 62.4% of the time needed by a single robot.

## VII. CONCLUSION

This article presented a 3-D mapping distributed architecture model for a team of cooperative mobile robots, which enables

to share efficiently sensory data and coordinate the exploration, using minimal communication. An exploration method was proposed whereby each robot selects exploration viewpoints with high entropy gradient, located in the frontier between explored and unexplored regions. Moreover, in order to coordinate exploration, each robot minimizes the mutual information between its visible map and the other robots' visible map, and also the interference with other robots, so that robots explore different map's regions and the map's uncertainty is decreased as fast as possible. Results obtained with real robots equipped with stereo-vision demonstrated that the entropy gradient-based method nicely converges to a map with lower uncertainty. The presented work is being extended with further experiments to better demonstrate the improvement of team's performance due to the coordination yielded by the proposed exploration method.

## REFERENCES

- [1] T. Arai, E. Pagello, and L. Parker. Special issue on advances in multirobot systems. *IEEE Tr. on Rob. and Autom.*, 18(5):655–864, 2002.
- [2] S. Thrun. Robotic mapping: a survey. In G. Lakemeyer and B. Nebel, editors, *Exploring Artificial Intelligence in the New Millenium*. Morgan Kaufmann, 2002.
- [3] C. Stachniss and W. Burgard. Mapping and exploration with mobile robots using coverage maps. In *Proc. of IEEE/RSJ Int. Conf. on Intelligent Robots and Systems (IROS'2003)*, pages 467–472, 2003.
- [4] S. Thrun, D. Hahnel, D. Ferguson, M. Montermelo, R. Riebwel, W. Burgard, C. Baker, Z. Omohundro, S. Thayer, and W. Whittaker. A system for volumetric robotic mapping of underground mines. In *Proc. of IEEE Int. Conf. on Robotics and Automation (ICRA'03)*, 2003.
- [5] M. Maimone, L. Matthies, J. Osborn, E. Rollins, J. Teza, and S. Thayer. A photo-realistic 3-D mapping system for extreme nuclear environments: Chernobyl. In *Proc. of IEEE/RSJ Int. Workshop on Intelligent Robots and Systems (IROS'98)*, volume 3, pages 1521–1527, 1998.
- [6] B. Yamauchi. Frontier-based exploration using multiple robots. In *Proc. of 2<sup>nd</sup> Int. Conf. on Autonomous Agents*, pages 47–53, 1998.
- [7] W. Burgard, M. Moors, D. Fox, R. Simmons, and S. Thrun. Collaborative multi-robot exploration. In *Proc. of IEEE Int. Conf. on Robotics and Automation (ICRA'00)*, volume 1, pages 476–481, 2000.
- [8] K. Konolige, D. Fox, C. Ortiz, A. Agno, M. Eriksen, B. Limketkai, J. Ko, B. Morisset, D. Schutz, B. Stewart, and R. Vincet. Centibots: very large scale distributed robotic teams. In *Proc. of Int. Symp. on Experimental Robotics, Singapore*, 2004.
- [9] M. Dissanayake, P. Newman, S. Clark, H. Durrant-Whyte, and M. Csorba. A solution to the simultaneous localization and map building (SLAM) problem. *IEEE Trans. on Robotics and Automation*, 17(3):229–241, 2001.
- [10] D. Hahnel, W. Burgard, D. Fox, and S. Thrun. An efficient FastSLAM algorithm for generating maps of large-scale cyclic environments from raw laser range measurements. In *Proc. of IEEE/RSJ Int. Conf. on Intelligent Robots and Systems (IROS'03)*, 2003.
- [11] F. Bourgault, A. Makarenko, S. Williams, B. Grocholsky, and H. Durrant-Whyte. Information based adaptive robotic exploration. In *Proc. of IEEE/RSJ Int. Conf. on Intelligent Robots and Systems (IROS'02)*, pages 540–545, 2002.
- [12] W. Burgard, D. Fox, and S. Thrun. Active mobile robot localization by entropy minimization. In *Proc. of 2<sup>nd</sup> Euromicro Workshop on Advanced Mobile Robots (EUROBOT'97)*, 1997.
- [13] C.E. Shannon. *The Mathematical Theory of Communication*. University of Illinois Press, 1949.
- [14] T. Cover and J. Thomas. *Elements of Information Theory*. Wiley Series in Telecommunications. John Wiley & Sons, 1991.
- [15] R. Rocha, J. Dias, and A. Carvalho. Entropy-based 3-D mapping with teams of cooperative mobile robots: a simulation study. Technical report, ISR, University of Coimbra, Portugal, Feb. 2004. [http://thor.deec.uc.pt/~rprocha/publications/040209\\_techReport2.pdf](http://thor.deec.uc.pt/~rprocha/publications/040209_techReport2.pdf).
- [16] R. Rocha, J. Dias, and A. Carvalho. Cooperative multi-robot systems for vision-based 3-D mapping using information theory. In *Proc. of Int. Conf. on Robotics and Automation (ICRA'05)*, Barcelona, Spain, 2005.

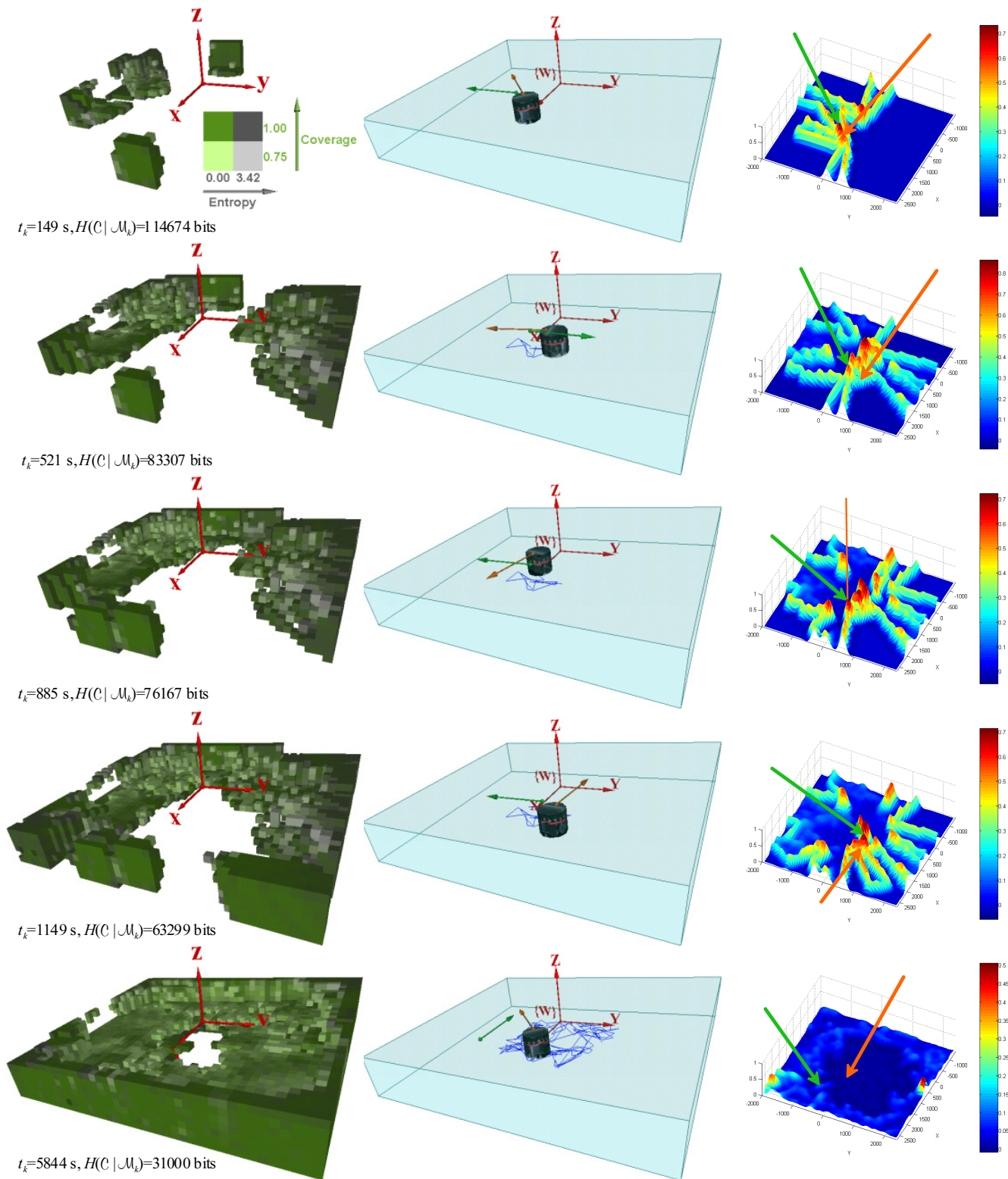


Fig. 6. Results obtained within an experiment with two Scout robots. The five rows represent the map's status of a robot at different instant times  $t_k$  with decreasing values of the map's entropy  $H(C | \mathcal{M}_k)$ . The left column depicts a VRML model of current 3-D map in the world reference frame (red referential). The middle column shows the current robot's sensor pose – orange arrow – and its next exploration viewpoint – green arrow – within the volume being explored. The arrows' origin indicates the position and their direction indicates orientation. The middle column also shows a blue polyline drawn in the floor plane, whose vertexes indicate the sequence of the robot's positions since the beginning of the mission. The right column depicts a graph of the normalized entropy gradient magnitude of voxels belonging to the sensor's motion plane  $\Gamma$  as a function of the voxels' center xy coordinates (expressed in millimeters). The orange and green arrows point to the current position of robot's sensor and its next exploration point, respectively. The scale of the pictures in the left and middle columns is such that each represented arrow (red, orange or green) is equivalent to a real length of 1 meter.